Chapter 5

Analyses of 316 test beams. Application of Artificial Neural Networks.

In order to take into account, in addition to our test results, the large amount of information available, a database with 316 test beams was assembled. The shear-span-to-depth ratio, *a/d*, for all of these beam specimens, is greater than 2.48, and all of them failed in shear. Other important parameters affecting the database are discussed later in §5.1.

The test results are compared with failure shear strengths predicted by the EHE Code, the Final Draft of the Eurocode 2, the AASHTO LRFD Specifications, ACI Code 318-99, and the Response-2000 program. Furthermore, two Artificial Neural Networks (ANNs) were developed for predicting empirical results and a parametric study was carried out based on the ANNs' predictions.

5.1 Introduction to the Experimental Database

The database used for these analyses relies on the databases developed by Bentz (2000) and Kuchma and Su (2002). However, more than 30 new tests were added, and many experimental campaigns carried out during the 1950's and 1960's have been omitted as

the reinforcement steel had a very low yielding stress. The final database contained 195 beams without shear reinforcement and 123 beam specimens with stirrups.

Table 5.1 gives a classified summary of the test beams. Detailed inputs and results of this experimental verification study are given in Annex C.

Although great efforts were made in order to achieve a homogeneous database, most beams had an effective depth that was too small and a longitudinal reinforcement that was too large. For instance, only 11% of the data without shear reinforcement had an effective depth greater or equal to 600 mm. This percentage is very similar for beams with stirrups (10%). Only 19% and 2% respectively of the beams contained an amount of longitudinal reinforcement equal to or less than 1%.

However, with the aim of reducing the influence of the database's lack of heterogeneity, the analyses were performed not only on the full set of beams, but also on partial subsets of the database. This allowed us to characterise the deficiencies of each procedure.

5.2 Verification of different shear procedures

Statistics for the two general databases are summarised in Table 5.2. It is important to mention that in this chapter the statistical analyses follows the modus operandi suggested by Collins (2001), which considers that the frequency distribution of V_{test}/V_{pred} is unsymmetrical, with a median value lower than the average. The values given in Table 5.2 are:

- The average value of V_{test}/V_{pred}. This is a measure of the conservative bias of the design procedure.
- The median value of V_{test}/V_{pred}, that divides the data into upper and lower 50%.
- The standard deviation of V_{test}/V_{pred} and its coefficient of variation (COV). These are indicators of accuracy.

Reference	num	d (mm)	f_c (MPa)	ρ_l (%)	ρ_w (MPa)	a/d
Beams without web reinforcement						
Morrow et al. (1957)	12	356 to 375	15 to 46	1.83 to 3.83	-	2.8 to 7.9
Elzanaty et al. (1986)	11	273	21 to 79	1.00 to 3.30	-	4.0 and 6.0
Mphonde et al.(1984)	12	298	22 to 102	2.32 and 3.36	-	2.5 and 3.6
Islam et al.(1998)	10	203 to 207	27 to 83	2.02 to 3.22	-	2.9 to 3.9
Collins et al (1999)	21	110 to 925	36 to 99	0.50 to 1.03	-	2.5 to 3.1
Ahmad et al. (1986)	14	184 to 208	61 to 67	1.77 to 6.64	-	2.7 to 4.0
Yoon et al. (1996)	3	655	36 to 87	2.8	-	3.23
Ahmad et al. (1994)	2	216	40 and 89	1.04 and 2.07	-	3.0
Kim et al. (1994)	16	142 to 915	54	1.01 to 4.68	-	3.0 and 4.5
Bazant et al. (1991)	18	41 to 165	46	1.62 and 1.65	-	3.0
Thorenfeldt et al(1990)	16	150 and 300	54 to 98	1.82 and 3.23	-	3.0 and 4.0
Kani et al. (1979)	32	137 to 1090	17 to 30	0.50 to 2.84	-	2.5 to 6.8
Cladera (2002)	4	359	50 to 87	2.24	-	3.0
Adebar et al. (1996)	6	178 and 278	46 to 59	1.0 to 3.04	-	2.9 and 4.5
Johnson et al. (1989)	1	610	56	2.49	-	3.1
Ahmad et al. (1995)	2	178	77 and 79	1.39	-	3.7
Xie et al. (1994)	2	216	38 and 99	2.07	-	3.0
Salandra et al. (1989)	4	171	52 to 69	1.45	-	2.6 and 3.6
Kulkarni et al. (1998)	3	152	42 to 45	1.37	-	3.5 to 5
González (2002)	4	305 and 306	40 to 47	2.9	-	2.3
Beams with shear reinforcement						
Angelakos (1999)	5	925	21 to 80	0.5 and 1.0	0.46	2.7
Yoon et al. (1996)	9	655	36 to 87	2.8	0.34 to 0.99	3.2
Collins et al. (1999)	2	920 and 925	71 and 47	1.03 and 0.75	0.78 and 0.36	5.0 and 2.92
Roller et al. (1990)	6	559 to 871	72 to 125	1.52 to 2.88	0.33 to 1.07	3
Adebar et al. (1996)	5	278	49 to 51	1.95	0.47 to 1.20	2.9
Tan et al. (1995)	4	397 to 463	43 to 74	1.23 to 2.00	1.85 to 2.58	2.8 to 3.1
Kong et al. (1998)	35	292 to 299	64 to 89	1.65 to 4.46	0.43 to 1.25	2.5 to 3.3
Johnson et al. (1989)	7	540	36 to 72	2.49	0.34 to 0.74	3.1
Ozcebe et al. (1999)	11	310	58 to 82	2.59 to 4.43	0.33 to 1.15	3.0 and 5.0
Cladera (2002)	12	351 and 353	50 to 87	2.28 and 2.99	0.58 to 1.29	3.1
Lyngberg (1976)	2	540	26 and 27	3.88	3.57 and 3.43	2.8
Ahmad et al. (1994)	4	198 and 216	45 to 88	2.07 to 4.54	1.59 to 3.28	3.0 and 4.0
Sarsam et al. (1992)	6	233	70 to 80	2.81 and 3.50	0.49 to 0.98	2.5 and 4.0
Etxeberria (2002)	3	303	42	2.99	0.62 to 1.15	3.30
González (2002)	12	302 to 312	38 to 45	2.86 to 2.99	0.60 to 1.05	3.21 to 3.30

Table 5.1: Summary of beams in database

- $COV_{LOW\ 50\%}$ is the coefficient of variation of a fictitious dataset formed by the lower 50% of the data and their symmetrical values around the median, resulting in a symmetrical distribution with an identical number of data to the original set. This parameter will be used for the calculation of the theoretical $(V_{test}/V_{pred})_{1\%}$ value that is introduced below.
- $COV_{HIGH\ 50\%}$ is identical to the previous value but with the highest 50% values. Note that the coefficients of variation for the 'high data set' are significantly higher than for the 'low data set', and for this reason the use of this technique is recommendable to obtain realistic theoretical 99% and 1% values.
- $(V_{test}/V_{pred})_{min}$. The minimum value in the database.
- $(V_{test}/V_{pred})_{1\%}$ is the theoretical value of the V_{test}/V_{pred} ratio of which 99% of the predictions can be expected to be higher. It is calculated using the following expression:

$$\left(\frac{V_{test}}{V_{pred}}\right)_{1\%} = \left(\frac{V_{test}}{V_{pred}}\right)_{median} \left(1 - 2.3 \cdot COV_{LOW\ 50\%}\right) \tag{5.1}$$

  where $COV_{LOW\ 50\%}$ is the coefficient of variation of a dataset formed by the lower 50% of the data and their symmetrical values around the median, resulting in a symmetrical distribution with an identical number of data to the original one.
- $(V_{test}/V_{pred})_{max}$. The maximum value of the ratio existing in the database.
- $(V_{test}/V_{pred})_{99\%}$. The theoretical value of the V_{test}/V_{pred} ratio of which 99% of members can be expected to be lower in value. It is calculated as follows:

$$\left(\frac{V_{test}}{V_{pred}}\right)_{1\%} = \left(\frac{V_{test}}{V_{pred}}\right)_{median} \left(1 + 2.3 \cdot COV_{HIGH\ 50\%}\right) \tag{5.2}$$

An exhaustive discussion of the results in Table 5.2 is presented later, and in this section we limit ourselves to making some important remarks. Figures 5.1 and 5.2 give the value of $(V_{test}/V_{pred})_{1\%}$. and $(V_{test}/V_{pred})_{99\%}$ for the analysed procedures. It can be seen in these figures that for members without web reinforcement, the ACI 11-3 equation presents the worst results, as it reaches both the minimum $(V_{test}/V_{pred})_{1\%}$ and the

maximum $(V_{test} / V_{pred})_{99\%}$. For members with web reinforcement EC-2 yields the worst correlation with the empirical results.

The results shown in Table 5.2 indicate that for members without shear reinforcement the proposed Eurocode 2 procedure is the least conservative procedure, with an average V_{test}/V_{pred} of 1.02, a median of 0.99, and COV equal to 22.03%. The best code performance is obtained by the AASHTO LRFD Standards. The average V_{test}/V_{pred} ratio is 1.28 and its COV is equal to 16.80%. The ACI 11-3 equation, which was used in Spain until 1999, shows the worst correlation with the studied beams. Its theoretical $(V_{test}/V_{pred})_{1\%}$ value is as low as 0.36.

Procedure	EHE	EC-2	AASHTO	ACI 11-5	ACI 11-3	Resp-2000
Beams without web reinforcement						
Average	1.23	1.02	1.28	1.28	1.29	1.13
Median	1.16	0.99	1.25	1.27	1.25	1.08
Standard deviation	0.29	0.23	0.22	0.34	0.40	0.23
COV (%)	23.61	22.03	16.80	26.36	31.21	20.00
$COV_{LOW\ 50\%}$ (%)	14.83	17.16	12.56	25.17	27.43	12.72
$COV_{HIGH\ 50\%}$ (%)	33.17	27.71	21.34	27.67	36.59	27.5
Minimum	0.78	0.57	0.86	0.47	0.42	0.73
$(V_{test} / V_{pred})_{1\%}$	0.76	0.60	0.89	0.54	0.46	0.76
Maximum	2.35	1.78	2.14	2.34	2.47	1.97
$(V_{test} / V_{pred})_{99\%}$	2.04	1.62	1.86	2.08	2.31	1.75
Beams with web reinforcement						
Average	1.64	1.83	1.18	1.36	1.41	1.07
Median	1.62	1.72	1.17	1.37	1.42	1.06
Standard deviation	0.43	0.74	0.23	0.34	0.38	0.19
COV (%)	26.26	40.29	19.23	24.60	26.70	17.39
$COV_{LOW\ 50\%}$ (%)	23.61	31.05	17.13	23.60	25.91	14.21
$COV_{HIGH\ 50\%}$ (%)	29.40	53.18	21.71	25.52	27.23	20.64
Minimum	0.62	0.50	0.69	0.69	0.67	0.75
$(V_{test} / V_{pred})_{1\%}$	0.74	0.49	0.71	0.63	0.57	0.71
Maximum	3.27	4.85	1.96	2.66	2.83	1.73
$(V_{test} / V_{pred})_{99\%}$	2.72	3.83	1.75	2.17	2.31	1.56

Table 5.2: Verification of shear procedures with full database.

The comparison with the 123 beams with shear reinforcement gives a greater scatter of results. It is quite surprising that, the latest procedure to be included in a code, the 2002

Final Draft of Eurocode 2, offers the worst results, with a very low accuracy, presenting the lowest minimum and the highest maximum results. Once again, the AASHTO LRFD Specifications show the best agreement with empirical values, with an average V_{test}/V_{pred} equal to 1.18 and a coefficient of variation of 19.23%. The worst correlation is the one obtained by calculating with the proposed Eurocode 2. Its average V_{test}/V_{pred} ratio is 1.72 and its COV up to 40.29%.

The Response-2000 program presented a satisfactory correlation for both sets of beams, although it was slightly better for beams with web reinforcement.

Collins (2001) proposed a 'Demerit Points Classification' to study the performance of different shear design procedures. It is based on assigning a 'mark' (DP, Demerit Point) to each range of V_{test}/V_{pred} values, as indicated in Table 5.3. The 'Total Demerit Point' score is calculated by summing the products of the percentage of each range multiplied by the Demerit Points for that range. This is based on the idea that it is 'worse' to have a V_{test}/V_{pred} lower than 0.50 than greater than 2.0.

The Total Demerit Points shown in Table 5.3 are plotted in Figures 5.3 and 5.4. Response 2000 gets the lowest score both for beams with and beams without web reinforcement, and therefore, gives the best performance, based on this criterion.

For beams without web reinforcement, the EHE Code and the AASHTO Specifications earn the same number of Demerit Points. The worst of the procedures analysed was equation 11-3 of the ACI Code.

For the set of beams with shear reinforcement, the AASHTO Code presents a very low number of Demerit Points compared to other specifications. The shear procedure published in the new draft of Eurocode gets the highest number of Demerit Points.

Both the Eurocode and EHE procedures earn a very different Demerit Point scores depending on the presence of shear reinforcement. Nevertheless, the Response-2000 program obtains the same score regardless of whether it is present.

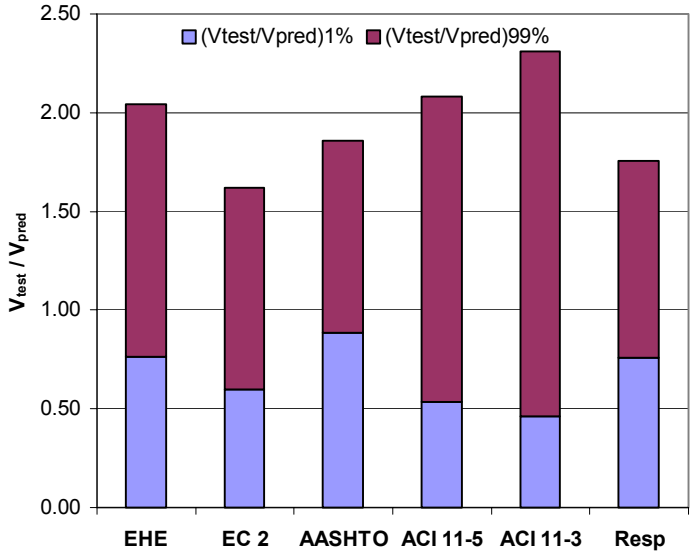

Figure 5.1: Verification of different code procedures. $(V_{test} / V_{pred})_{1\%}$ and $(V_{test} / V_{pred})_{99\%}$ for members without web reinforcement.

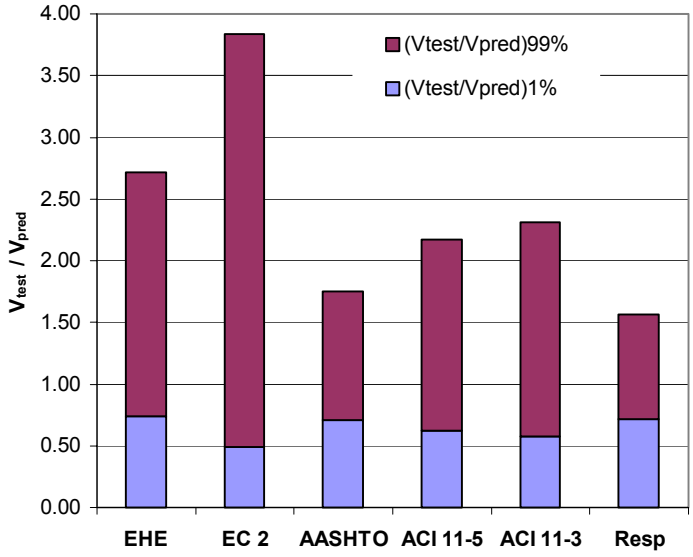

Figure 5.2: Verification of different code procedures. $(V_{test} / V_{pred})_{1\%}$ and $(V_{test} / V_{pred})_{99\%}$ for members with web reinforcement.

The results of the partial set analyses are shown in Table 5.4. We tried to study the size effect, the influence of the amount of longitudinal reinforcement, transversal reinforcement, and the concrete compressive strength separately.

$\frac{V_{test}}{V_{pred}}$	Classification	DP	EHE	EC-2	AASHTO	ACI 11-5	ACI 11-3	Resp
Beams without web reinforcement								
< 0.50	Extremely dangerous	10	0	0	0	1	2	0
0.50 - 0.65	Dangerous	5	0	3	0	2	2	0
0.65 – 0.85	Low safety	2	5	16	0	7	9	5
0.85 – 1.30	Appropriate safety	0	67	69	61	48	44	78
1.30 – 2.00	Conservative	1	26	12	39	40	37	17
> 2.00	Extremely conservative	2	2	0	1	2	6	0
Total Demerit Points			**40**	**59**	**41**	**78**	**97**	**27**
Beams with web reinforcement								
< 0.50	Extremely dangerous	10	0	1	0	0	0	0
0.50 - 0.65	Dangerous	5	1	2	0	0	0	0
0.65 – 0.85	Low safety	2	2	2	5	6	6	8
0.85 – 1.30	Appropriate safety	0	14	15	69	36	31	82
1.30 – 2.00	Conservative	1	69	48	26	56	58	10
> 2.00	Extremely conservative	2	14	32	0	2	6	0
Total Demerit Points			**106**	**136**	**36**	**72**	**82**	**26**

Table 5.3: Demerit Point Classification.

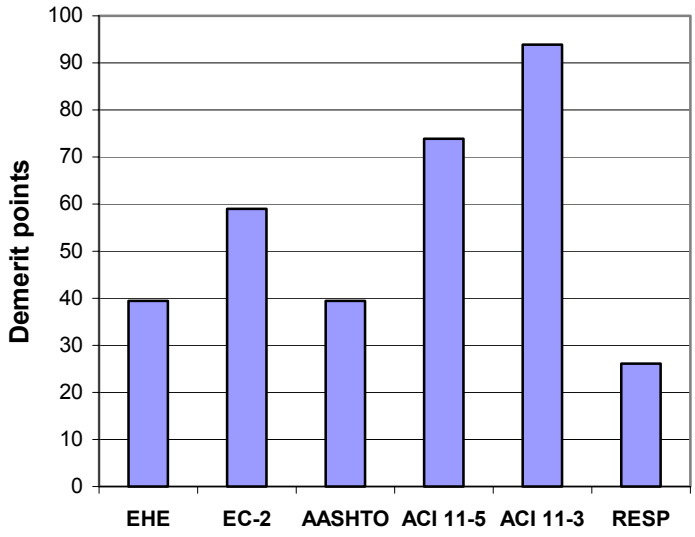

Figure 5.3: Verification of different shear design procedures. Demerit Points for beams without web reinforcement.

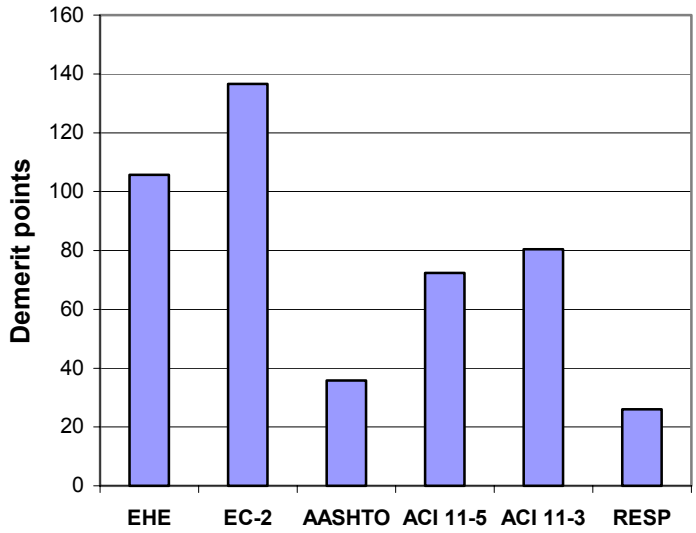

Figure 5.4: Verification of different shear design procedures. Demerit Points for beams with web reinforcement.

Beam specimens	nº beams	Average V_{test} / V_{pred}					COV V_{test} / V_{pred}				
		EHE	EC-2	AASHTO	ACI 11-5	ACI 11-3	EHE	EC-2	AASHTO	ACI 11-5	ACI 11-3
Beams without web reinforcement											
All	193	1.23	1.02	1.28	1.28	1.29	23.61	22.03	16.80	26.36	31.21
$d \geq 900$ mm	18	1.03	0.83	1.11	0.78	0.76	13.63	18.84	14.46	24.75	28.49
$d \leq 100$ mm	12	0.98	1.18	1.42	1.61	1.58	8.09	10.59	10.57	10.62	10.65
$\rho_l \leq 1\%$	37	1.09	0.89	1.16	0.97	0.90	14.49	17.40	10.13	23.81	25.51
$f_c > 50$ MPa	93	1.31	1.03	1.29	1.30	1.32	26.14	25.81	20.10	29.19	34.23
$f_c \leq 50$ MPa	100	1.15	1.01	1.28	1.27	1.27	17.86	17.58	12.99	23.36	27.79
$\rho_l > 2\%$ $f_c > 50$ MPa	55	1.46	1.15	1.38	1.47	1.54	23.54	23.24	19.85	22.63	26.27
$\rho_l > 2\%$ $f_c \leq 50$ MPa	34	1.31	1.10	1.35	1.43	1.52	16.50	16.10	13.26	17.22	20.68
Beams with web reinforcement											
All	123	1.64	1.83	1.18	1.36	1.41	26.26	40.29	19.23	24.60	26.70
$d \geq 750$ mm	12	1.29	1.34	1.00	0.91	0.88	16.22	24.66	20.38	18.73	20.97
$\rho_w \leq 1$MPa	93	1.71	2.05	1.18	1.37	1.42	24.60	34.28	19.84	26.01	28.42
$\rho_w > 1$MPa $\rho_w \leq 2$MPa	23	1.57	1.28	1.22	1.38	1.42	21.89	22.76	15.89	17.68	18.66
$\rho_w > 2$MPa	7	0.98	0.78	1.07	1.18	1.23	19.63	19.63	20.91	22.29	23.84
$f_c \leq 50$ MPa	38	1.47	1.44	1.13	1.30	1.33	22.01	29.70	17.99	22.48	23.71
$f_c > 50$ MPa	85	1.72	2.01	1.21	1.39	1.44	26.33	38.92	19.51	25.21	27.57
$\rho_l \leq 2$ %	19	1.24	1.33	0.99	0.98	0.96	17.97	32.24	15.54	21.60	23.37

Table 5.4: Verification of different code procedures using partial sets of the database

5.2.1 EHE Code

The performance of the EHE Code was very different for members with shear reinforcement from those without it. For the first dataset, the EHE correlates satisfactorily with the empirical results. On the other hand, for members with web reinforcement, the EHE Code is, in general terms, too conservative (Figure 5.5).

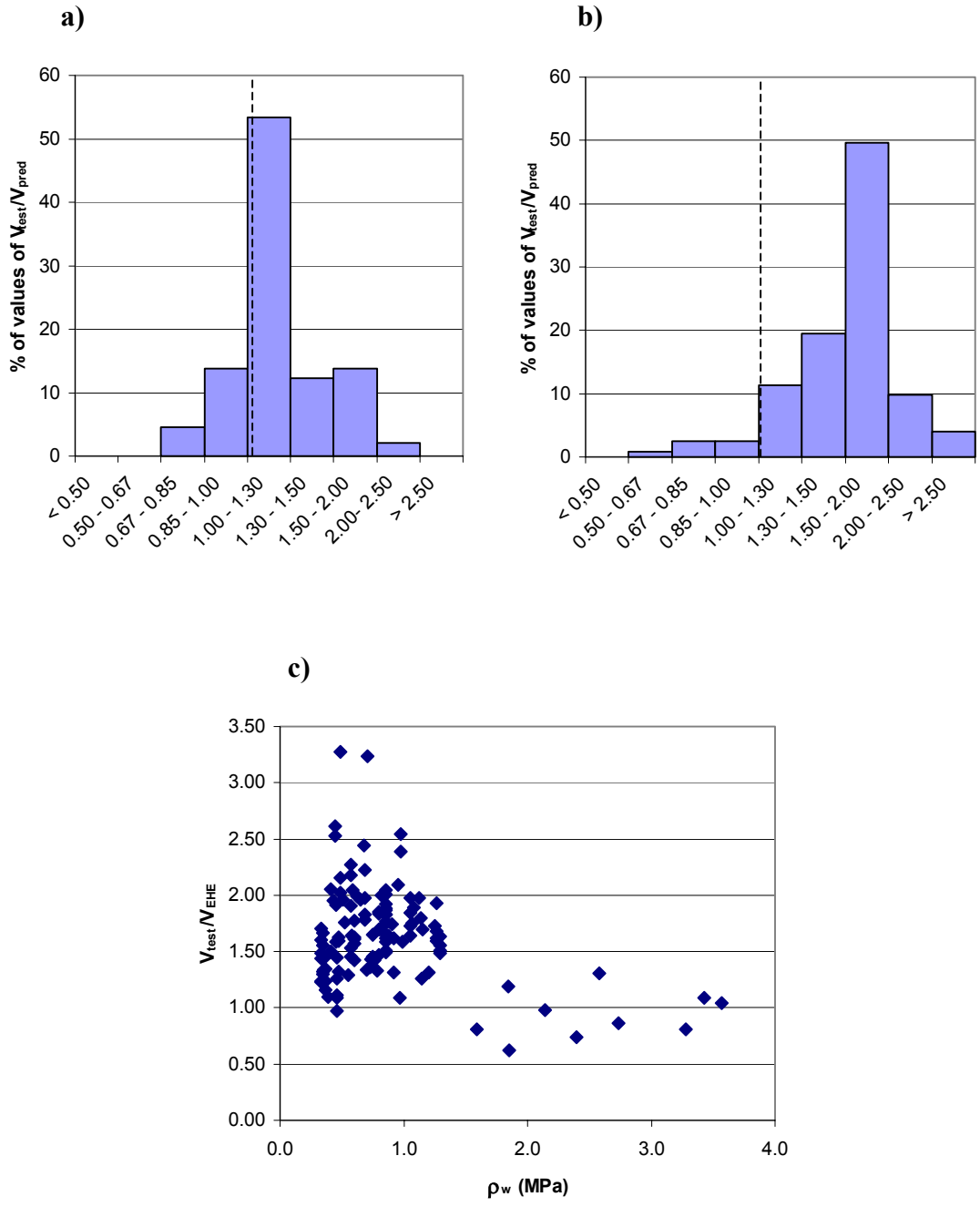

Figure 5.5: Correlation of the EHE procedure with empirical tests. a) Beams without web reinforcement. b) Beams with web reinforcement. c) Beams with web reinforcement. Influence of the amount of shear reinforcement

However, as shown in Table 5.4, the correlation is not identical for the different partial databases. For beams without web reinforcement, the safety is reduced for larger members ($d \geq 900$ mm), for small ones ($d \leq 100$ mm), and for elements with a low amount of longitudinal reinforcement ($\rho \leq 1\%$). In contrast, the average value of V_{test}/V_{pred} is higher for members with more than 2 % of longitudinal reinforcement, especially for high strength concrete beams.

For elements with web reinforcement, though this is a highly conservative procedure, the safety is reduced when the shear reinforcement is increased (Figure 5.6).

For high strength concrete beams the average V_{test}/V_{pred} ratio also increases relative to normal strength concrete beams.

5.2.2 Eurocode 2: April 2002 Final Draft

The Eurocode 2 procedure for members without web reinforcement is very similar to the EHE proposal, but more unconservative (§2.2.3). Moreover, it does not limit the value of the concrete compressive strength, and there is a maximum value of the size effect for small members. It generally correlates worse with the test results than the EHE Code does.

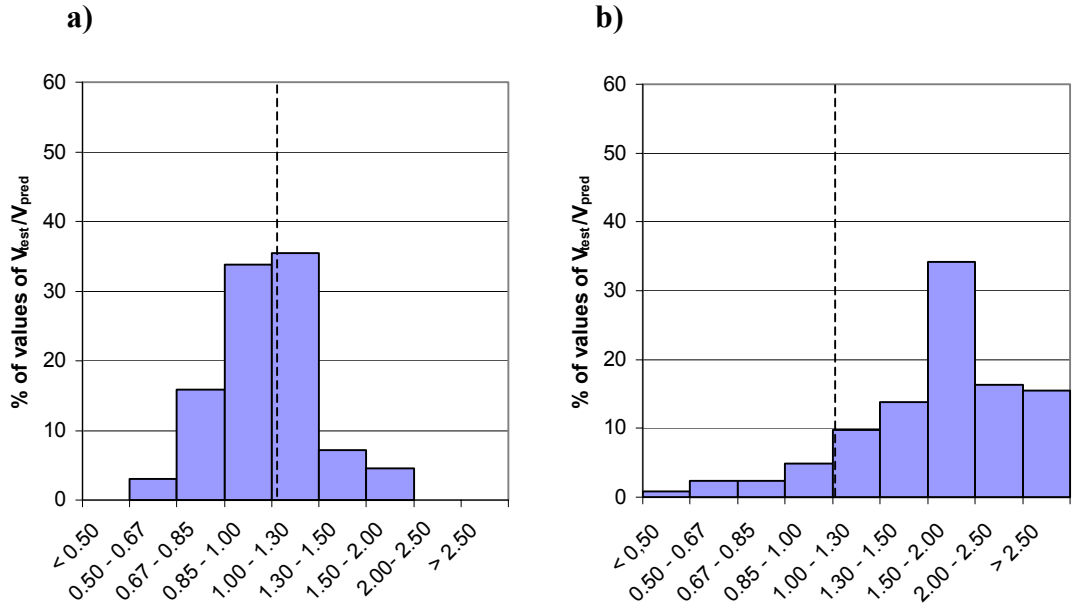

Figure 5.6: Correlation of the EC-2 procedure with empirical tests. a) Beams without web reinforcement. b) Beams with web reinforcement.

For members with web reinforcement, the proposed Eurocode procedure is based on a truss model in which $cot\theta$ can be as high as 2.5, and in which the concrete contribution is excluded. Figure 5.6.b demonstrates that this is a very unrealistic approach, as it produces extremely conservative results for some members and extremely dangerous ones for others. In fact, this procedure yields the lowest $(V_{test}/V_{pred})_{1\%}$ value and the highest $(V_{test}/V_{pred})_{99\%}$ value, as is shown in Figure 5.2. The Eurocode approach is compared to the AASHTO Specification procedure in Figure 5.7.

The most conservative results are predicted for members with a low amount of shear reinforcement and for small members, while the most unconservative predictions are calculated for highly reinforced members and larger members (Table 5.4).

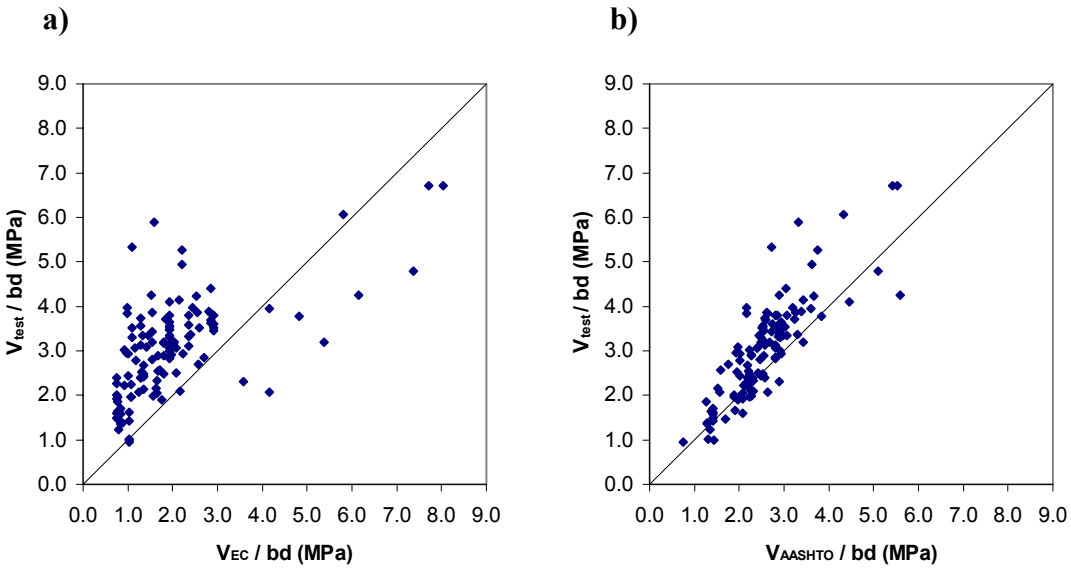

Figure 5.7: Comparison of shear procedures with empirical results for members with web reinforcement. a) Eurocode 2 –April 2002 Final Draft. b) AASHTO LRFD Specifications.

5.2.3 AASHTO LRFD Specifications

The AASHTO shear design procedure earns the best Demerit Point Classification both for members with and without shear reinforcement of all the codes of practice studied without taking into account Response 2000 program (Figures 5.3 and 5.4).

It may be slightly conservative for members without web reinforcement, but it is indeed a highly accurate procedure, as can be seen in Figure 5.8.a.

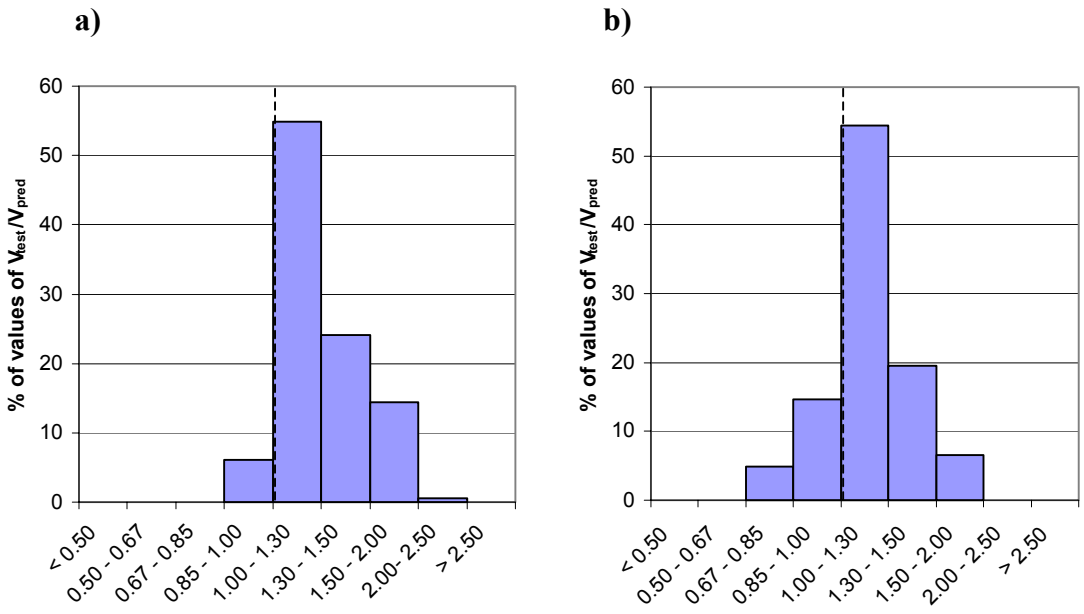

Figure 5.8: Correlation of the AASHTO LRFD shear procedure with empirical tests. a) Beams without web reinforcement. b) Beams with web reinforcement.

For members with web reinforcement, partial database analyses reveal that for larger members and for members with a low amount of longitudinal reinforcement the predicted values decrease their safety bias (Table 5.4).

The only disadvantage that this shear procedure may present is its lack of simplicity. Furthermore, it is intended to be a tool for designing, and one must use a short spreadsheet or iterate to check the failure shear strength for any given section (§2.3.6)

5.2.4 ACI Code 318-99

The ACI Code presents two different shear design methods depending on the concrete contribution used (§2.3.6 and §2.2.3). For members with stirrups the differences between the two methods are not very significant. The main differences are found in members without web reinforcement.

The percentages of results in different ranges of V_{test}/V_{pred} for both methods and members without shear reinforcement are given in Figure 5.9. The procedure based on equation 11-3 gives a very low prediction for some beam specimens. This equation was included in the Spanish EH-91 Code.

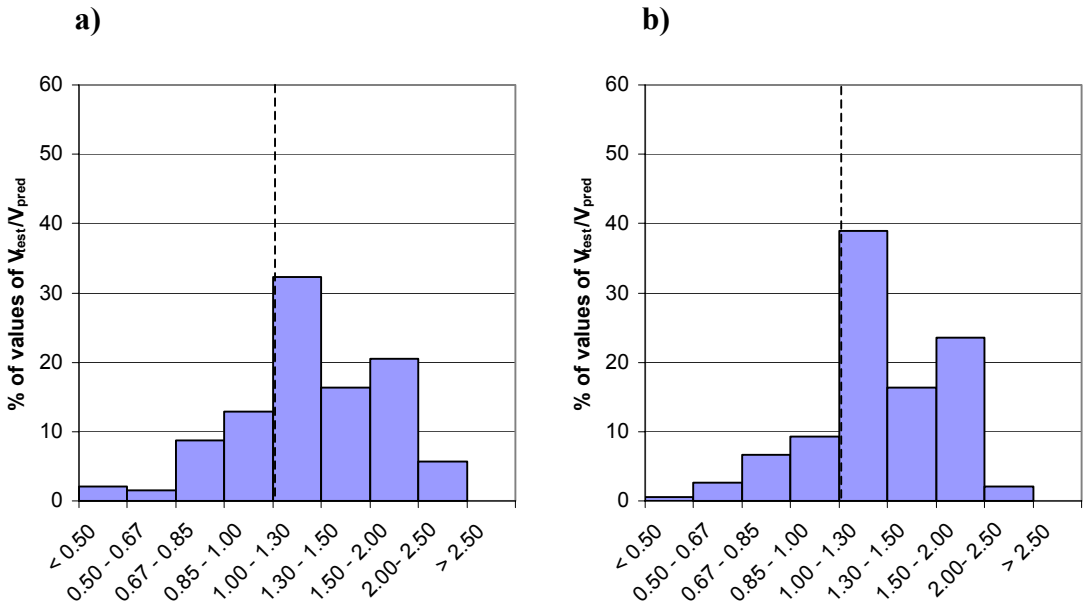

Figure 5.9: Correlation of the ACI Code shear procedures with empirical tests for beams without web reinforcement. a) Equation 11-3. b) Equation 11-5.

Equation 11-3 is particularly unconservative for larger members and for members with a low amount of longitudinal reinforcement. The average V_{test}/V_{pred} ratio is 0.76 for beams in which *d* is greater than 900 mm, and 0.90 for elements with an amount of longitudinal reinforcement lower than or equal to 1%.

The analyses carried out for members with shear reinforcement reveal that for the database utilised, these two methods correlate better with the empirical results than the EHE shear design procedure does, as they earn fewer Demerit Points (Figure 5.4) and have a lower standard deviation (Table 5.2). Nevertheless, it is compulsory to highlight that both procedures present a $(V_{test}/V_{pred})_{1\%}$ lower than the EHE method.

5.2.5 Response-2000

The Response-2000 program correlates satisfactorily for both sets of beams as can be seen in Figures 5.10.a and 5.10.b. For beams without web reinforcement the shear strength of 78% of the beam specimens is predicted within the appropriate safety. This percentage for the beams without web reinforcement goes up to 82%. Moreover, according to the classification laid out in Table 5.3, none of the predicted values gives a dangerous or extremely conservative estimation of the shear strength.

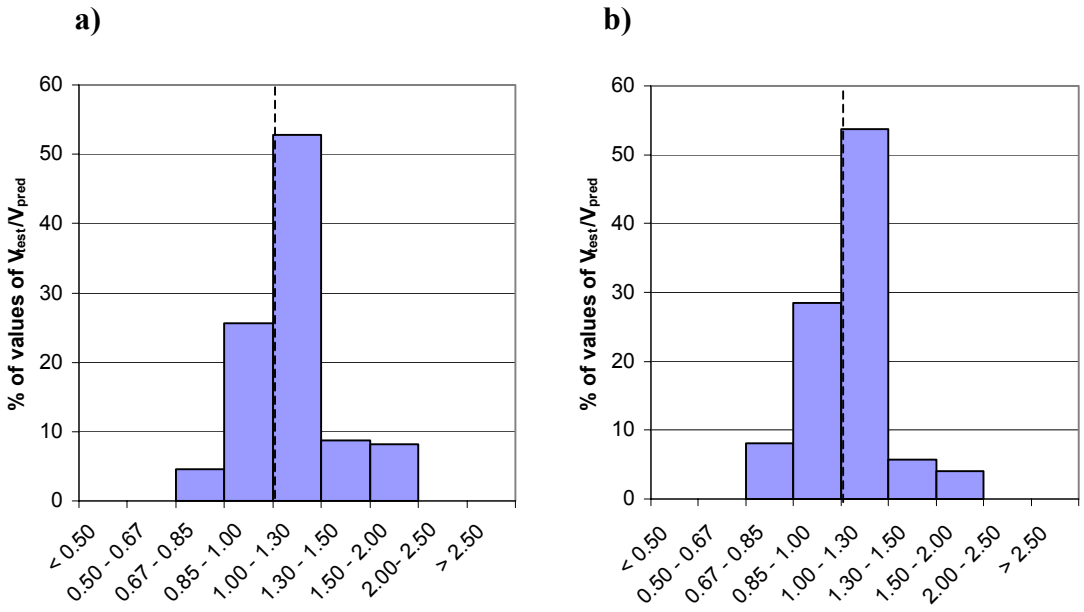

Figure 5.10: Correlation of the Response 2000 predictions with empirical tests. a) Beams without web reinforcement. b) Beams with web reinforcement.

5.3 Introduction to Artificial Neural Networks

An Artificial Neural Network (ANN) is a computational tool that attempts to simulate the architecture and internal features of the human brain and nervous system (Sanad et al. 2001). ANNs are made up of a number of simple, highly-interconnected processing elements, representing neurons, that constitute a network. Each neuron receives several inputs from neighbouring elements, but only sends one output. The training process of an ANN involves presenting a set of examples with known inputs and outputs. The system adjusts the weights of the internal connections to minimise errors between the network output and target output. Moreover, this learning occurs even when the input data contains errors or is incomplete, which is one of the problems we must address when talking about shear strength. An excellent reference about neural network design for engineering applications is Rafiq et al. (2001).

Figure 5.11 represents a typical ANN configuration. The function of an input layer is to receive information from the outside world. The hidden layer links the input layer to the output layer, and the output layer communicates the ANN result to the outside world.

Two different neural networks have been built to predict the ultimate shear strength for beams without and with web reinforcement respectively. The program PDP++ (2002 updated) by O'Reilly et al. from Carnegie Mellon University was used.

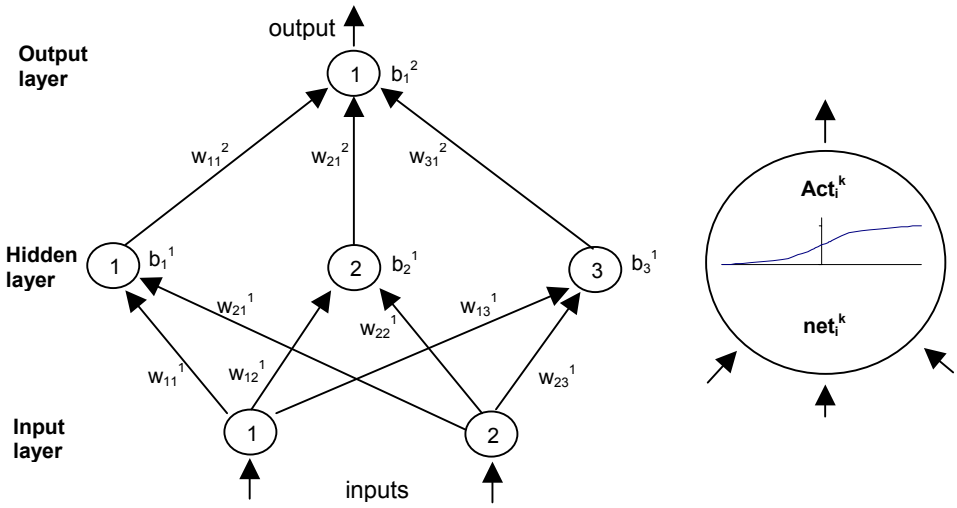

Figure 5.11. Typical neural network model. Adapted from Sanad and Saka (2001).

5.3.1 The Human Neural Network vs. Artificial Neural Networks.

Although Artificial Neural Networks try to simulate some characteristics of the human nervous system, their real behaviour is quite different.

A human neural network is made of billions of nerve cells, or neurons. Each neuron has dendrites (inputs), a cell body and an axon (output) as can be seen in Figure 5.12. A neuron receives inputs from other neurons and if the 'average' input exceeds a critical level, the neuron discharges an electrical pulse that travels from the body down the axon to the next neuron or group of neurons. These three main parts of a biological neuron are reproduced in an artificial neuron. It receives inputs (dendrites), operates in reaction to them (body cell), and sends an output (axon).

The human brain contains about 10 billion neurons. Each neuron is connected to some thousand other neurons, forming a massively parallel information processing system. On the other hand, conventional computers contain a processor that executes a single series of instructions. In fact, the brain is built with very slow 'hardware', as neurons typically operate at a maximum rate of about 100 Hz (Schraudolph and Cummins,

2001), in marked contrast to a conventional CPU, which is able to carry out several hundred million operations per second.

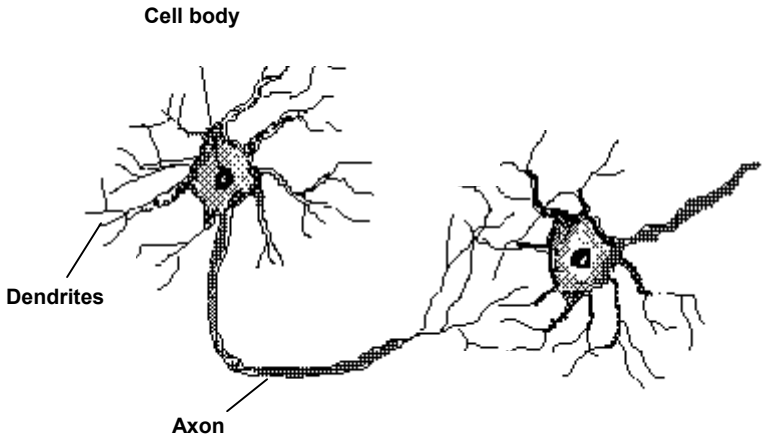

Figure 5.12. Human neuron. An artificial neuron tries to reproduce its three main parts.

Though a parallel processing system together with a very high number of connections offers capabilities remarkably similar to the human brain (Schraudolph and Cummins, 2001), it cannot replicate exactly the following characteristics:

- Under partial damage the performance of the brain tends to degrade gracefully. In contrast, computers usually cease to function when a small part is damaged.

- It can learn from experience (reorganising itself).

- It can partially recover from damage if healthy neurons learn to take over the functions previously carried out by damaged areas.

- It can perform massively parallel computations extremely efficiently. For instance, researchers say that complex visual perception occurs within less than 100 ms, that is, less than 10 processing steps.

The learning process is also highly simplified in Artificial Neural Networks. The brain learns online, based on experience, and normally without supervision. During this process, the strength of connections between neurons changes, and some connections are added or deleted. Learning in Artificial Neural Networks is based on adjusting the

weights of previously established internal connections to satisfactorily reproduce a training pattern of data. The learning process is generally controlled by the computer user.

5.3.2 Building an Artificial Neural Network.

To build an Artificial Neural Network one must define all the different elements involved:

- The type of neuron.
- The number of neurons in the input layer.
- The number of hidden layers and number of neurons in the hidden layer/s.
- The number of neurons in the output layer.
- The connections between neurons and layers.

In fact, almost every stage of the construction of a neural network involves some trial and error to establish a suitable network architecture and an optimum level of training. Let us take this step by step.

Neuron type

The artificial neuron is the basic computational unit. As has been seen earlier, it receives inputs either from other units or from the outside world. Each input has an associated weight *w* (see Figure 5.11), which will be modified during the learning process. Sometimes there is also a constant value, or bias, that is added to the input signals. The unit then calculates the net input, which is a weighted sum of its inputs plus the bias value:

$$net_i = \sum w_{ij} A_j + b_i \tag{5.3}$$

Next, the neuron computes some function f of the net_i value, named the activation function. The result is called the activation value. The net value ranges from -∞ to +∞. In contrast, the activation value usually ranges from –1 to +1 or 0 to +1.

Different activation functions can be used, and therefore, different neurons be utilised. The most 'primitive' activation function will give zero for all net values unless they exceed a certain threshold level. In the second case the activation value will be equal to 1. This type of activation function was used in the first versions of Artificial Neural Networks (Torras et al. 1998), as it reproduces the behaviour of human networks. However, its performance during the learning process was not very good, and other activation functions were developed.

The most common type of activation function used in engineering applications is the sigmoid transfer function, shown in Figure 5.13, whose equation is as follows:

$$A_i = \frac{1}{1 + e^{-net_i}} \tag{5.4}$$

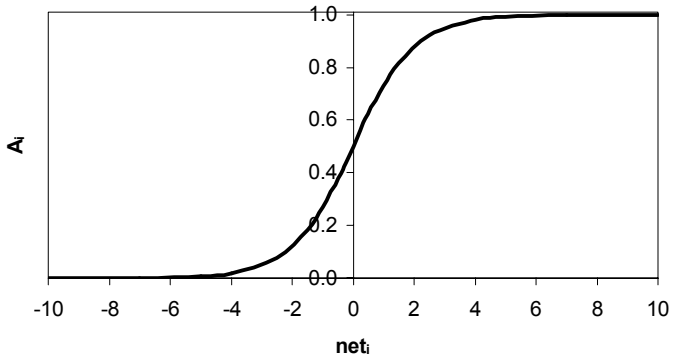

Figure 5.13: Sigmoid transfer function.

Input layer

The input layer must receive inputs from the outside world. Too many input parameters will drastically slow down the learning process. However, for our problem, the number of input parameters is quite well defined by the problem itself, and the parameters considered are the same as those taken into account by different codes.

In Section 5.4 and 5.5, the input parameters used respectively for the ANNs for beams with and without web reinforcement are discussed.

Hidden layer

The function of the hidden layer is to extract and remember useful features and subfeatures from the input patterns to predict the outcome of the network. Some authors suggest (Rafiq et al. 2001) that for continuous functions a single hidden layer with a sufficient number of neurons will be suitable while a second layer will be needed for discontinuous problems.

The number of neurons in the hidden layer will be defined by a process of trial and error. If too few processing units are considered then the artificial network will not be able to learn satisfactorily and the response of the network to unseen data will be poor. On the other hand, too many hidden neurons will produce over-fitting (Figure 5.14), and the solution surface produced by the network may develop false features at points between training patterns. This may be particularly dangerous for patterns of data with some noise, such as our data from the test beams. In general, a smooth interpolation between training data is sought.

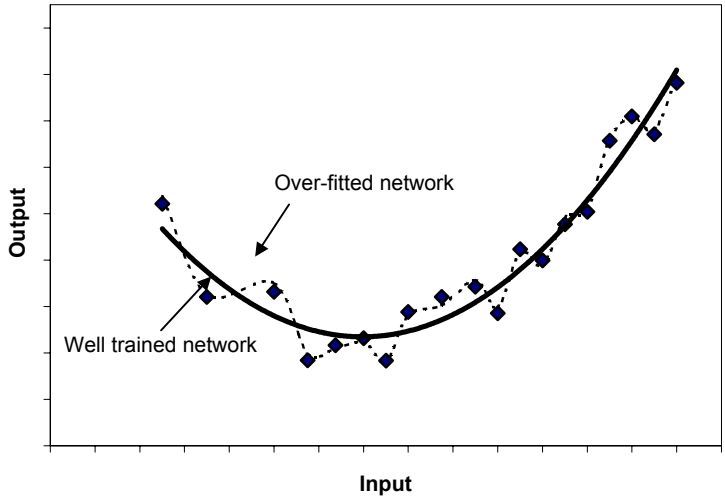

Figure 5.14: Example of an over-fitted network vs. a well-trained network. Adapted from Schraudolph et al. (2002).

Output layer

The function of the output layer is to output the result of the ANN to the outside world. In general, an ANN could have many outputs, and the output layer would then be made up of several neurons. In the shear strength problem, the only output considered is the failure shear strength and therefore only one processing unit is considered in the output layer.

Connections between neurons

The neurons of an Artificial Neural Network may be interconnected in very different ways. One neuron may be connected to just few neighbouring neurons, to all the neurons in the previous layer, or to all the neurons in the network.

In the most common neural networks used in engineering problems each neuron is fully interconnected with the adjacent layers yet is not connected to the neurons on the same level. In these networks the information goes from the input layer to the output layer without any cycles. These networks are termed feed-forward networks (Figure 5.11).

5.3.3 Learning process: Back-propagation.

Once the network has been built, it is necessary to train it to adjust the weights of each connection. Learning in a feed-forward network involves the back-propagation of the network error obtained by comparing the output value and the target value of the training data.

The back-propagation algorithm can be found in any reference about Artificial Neural Networks, for example Torras et al. (1998), Schraudolph et al. (2002) or O'Reilly et al. (2002).

To summarise, the back-propagation algorithm is comprised of the following steps:

1. The internal weights are randomly initialised.

2. The network propagate the input values of the training data to obtain an output result for each data. This point will be discussed later in detail.

3. The output result is compared with the target value, and the error is then computed as the summed square error:

$$E = \sum_i \left(A_{i,target} - A_{i,output} \right)^2 \tag{5.5}$$

4. The error is back-propagated. The negative of the derivative of the error with respect to the activation and with respect to the net input to each unit is computed, starting at the output layer and passing successively back through successively lower numbers of layers.

5. Finally, the weights and biases are updated. In general, the following expression is used to calculate the increase in weight increment:

$$\Delta w_{ij} = l_{rate} \frac{\partial E}{\partial w_{ij}} + m \cdot \Delta w_{ij}^{previous} \tag{5.6}$$

where

l_{rate} is the learning rate, a constant which scales the size of the effect of the weight error derivative, and

m is the momentum parameter, which scales the extent to which previous weight changes carry through to the current weight change. This is actually an extension of the backprop algorithm, and it will help us to avoid local minimums, to prevent over-fitting and to speed up convergence.

6. Go to step number 2 and repeat the process until the network is satisfactorily trained. Each instance that the training data is presented to the network is known as an epoch. The number of epochs will affect the performance of the network.

The question raised now is when the training process stops. If the training is not carried out long enough, the network will not learn every feature and hence its network performance will be unsatisfactorily. It the network is trained for too long, it begins to over-fit and to model the noise of the training data (Figure 5.15).

One of the simplest and most widely used means of avoiding over-fitting is to divide the data into two sets: a training set and a validation or testing set. Testing trained networks at different intervals will avoid the pitfall of over-fitting and will thus produce a good network generalisation.

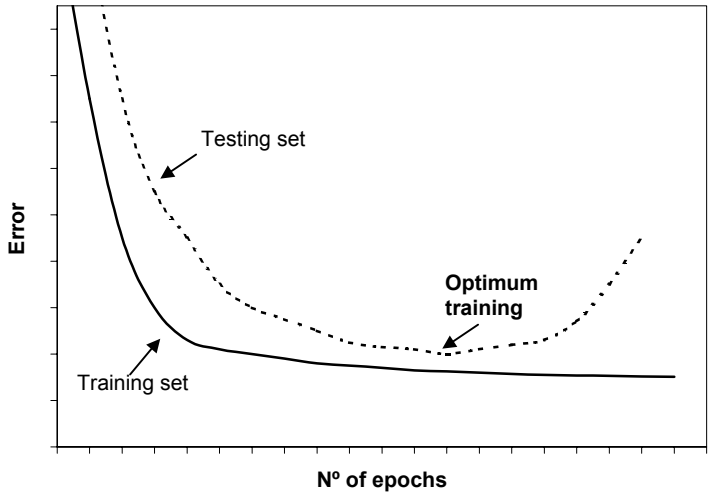

Figure 5.15: Typical learning curves showing the error on training and testing sets.

There are, generally speaking, two different modes of training an ANN using the back propagation algorithm: batch learning and online learning. In the batch mode, a single error is computed when the entire set of training data is presented to the network and the weights in the network are updated according to that error. In the alternative online or 'pattern' mode, the weights are updated immediately after reading each data point. Whichever method is chosen, it will condition what action is taken in the step two of the previous list.

There is no general rule for choosing between these two training modes. The batch mode requires less weight updates and hence may be faster to train, but it is also more likely to become trapped in local optima. Rafiq et al. (2001) suggest training the network using batch mode to start with and testing and analysing the network output. If the level of error after testing the network with unseen data was not satisfactory then a pattern mode should be used.

5.3.4 Data selection and pre-processing of the data

It has been seen that two sets of data are needed: a training set and a testing (or validating) set. To build the two Artificial Neural Networks we have used the database presented in §5.1. The validating set contains approximately 15% of the total database.

Many authors recommend removing some of the data outliers for better and smoother network generalisation, provided that these data are extreme and uncharacteristic of the problem domain.

Data scaling is also an essential step for training the network. As the sigmoid transfer function is used (Figure 5.13), scaling the input to the range of [0,+1] will greatly improve the learning speed (Rafiq et al. 2001). Moreover, the authors have found from experience that a better fit will be achieved if the normalised data is kept away from the sigmoid extreme boundaries of 1 and 0.

A simple linear normalisation between 0.2 and 0.8 can be used to scale the input values:

$$\hat{V} = 0.2 + 0.6\,\frac{V - V_{min}}{V_{max} - V_{min}} \tag{5.7}$$

where $\hat{V}$ is the scaled value of the variable V, and V_{min} and V_{max} are the variable minimum and maximum values respectively.

A different method is adopted by the author for normalising the output variables. As use of the square root function reduces the effect of outliers, the following expression is recommended:

$$\hat{V} = \left(\frac{V}{10^{n}}\right)^{1/2} + C \tag{5.8}$$

where n is the number of digits of the integer part of the variable V, and C is a constant used to ensure that the values fall between 0.2 and 0.8.

5.4 Artificial Neural Network for members not containing shear reinforcement

An ANN was developed to predict the failure shear strength of beams without web reinforcement. In this section it is described the data selection process, the topology of the constructed network, the training process and the verification of the ANN results. Finally, a parametric study is carried out in §5.4.4 based on the ANN predictions.

5.4.1 Data selection

In total, 177 test beams were used to train and test the Artificial Neural Network out of the 195 beams of the experimental database presented in §5.1. In other words, 18 beams had to be removed to ensure a satisfactory generalisation.

As was stated earlier, sometimes it may be necessary to remove the outliers for better generalisation. The 18 beams removed were those tested by Bazant et al. (1991) with a web width equal to 38.1 mm, much smaller than the next lowest width of 102 mm. Although it was initially tried to use these data, it was seen that the network performance was much better when they were removed.

The input parameters considered are the effective depth (d); the web slenderness factor d/b, where b is the web width; the a/d ratio; the reinforcement ratio of longitudinal tensile steel (ρ); and the concrete cylinder compressive stress (f_c). The output value is the failure shear strength V. Table 5.5 summarises the ranges of each different variable.

Parameter	Minimum	Maximum
d (mm)	101.6	1090
d/b	0.37	7.17
ρ (%)	0.50	6.64
f_c (MPa)	14.7	101.8
a/d	2.48	7.86
V (KN)	19.52	332.14

Table 5.5: Artificial Neural Networks for beams without web reinforcement. Range of parameters in the database.

The 177 test beams were divided into two sets: a training set containing 147 beams, and a validating set with 30 beams. The validating data were extracted more or less randomly, but following two criteria: both sets had to first present a similar average and coefficient of variation for the V_{test}/V_{pred} ratio, V_{pred} being the predicted shear strength for the beams as calculated by the codes analysed in this thesis; and second, had to try to avoid boundary parameters. Table 5.6 shows the correlation of the two sets of beams with the different shear procedures. It can be seen than the correlation is slightly better for the validating test. All the information related to the test beams in both sets is summarised in Annex C.

Beam specimens	nº beams	Average V_{test} / V_{pred}						COV V_{test} / V_{pred} (%)					
		EHE	EC-2	AASHTO	ACI11-5	ACI11-3	Resp	EHE	EC-2	AASHTO	ACI11-5	ACI 1-3	Resp
Training set	147	1.25	1.02	1.28	1.27	1.28	1.15	23.66	22.29	17.35	27.12	32.35	20.44
Validating set	30	1.24	1.01	1.24	1.24	1.25	1.08	22.99	24.37	15.81	26.47	33.23	19.46

Table 5.6: Artificial Neural Networks for beams without web reinforcement. Training and validating sets.

5.4.2 Topology of the Artificial Neural Network, learning process and validation.

A method of trial and error was carried out to define the optimum topology, learning procedure, and duration of the learning process. Some aspects were fixed from the beginning:

- 5 neurons in the input layer (d, d/b, a/d, ρ, and f_c).
- 1 neuron in the output layer (V).
- Feed-forward connections, based on other authors' experience.
- Activation function: Sigmoid transfer function (Figure 5.13).
- Momentum: 0.9.

To choose between pattern and online training, both methods were tested for a different number of hidden neurons. It was seen in our problem that online training resulted in a faster convergence at the beginning. Nevertheless, even though batch training was slower, it offered steadier results and a better generalisation.

Once we defined the learning procedure, Artificial Neural Networks with a different number of hidden neurons were trained with regular stops to check their behaviour. After checking more than 50 different trained networks, the best solution was obtained with a neural network containing 10 hidden units and after 8000 epochs. The learning rate varied to ensure convergence between 0.175 at the beginning of the training procedure and 0.08 for a high number of epochs. The final weights and biases that fully define the ANN are given in Annex D.

The summed square error per number of data in both sets is plotted in Figure 5.16 against the number of iterations or epochs for a ANN with 10 hidden neurons. While the error in the training set always decreases, there is a low point for the testing set. The final network, with 8000 epochs, shows a satisfactory generalisation, as the testing set event gives a lower error than the training set.

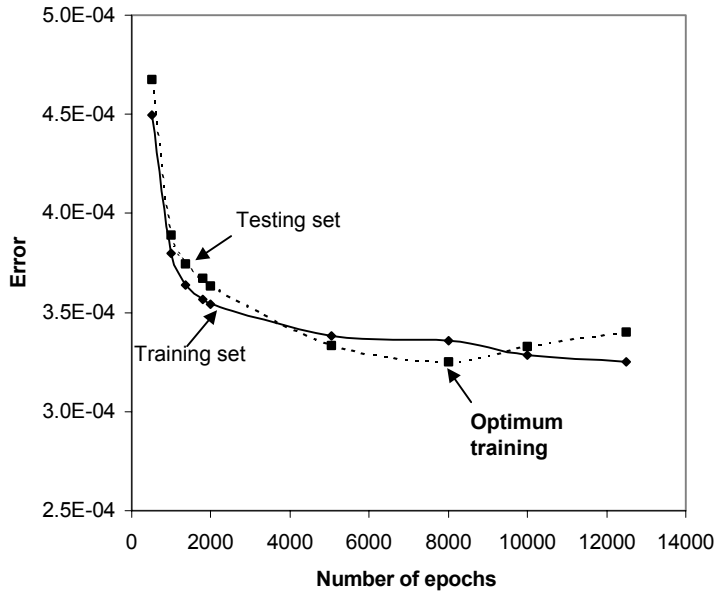

Figure 5.16: Artificial Neural Network for beams without web reinforcement. Learning process for network with 10 hidden units.

Being able to compare the Artificial Neural Network results with the code predictions is necessary to undo the pre-processing of the output value. Once this takes place, the average V_{test}/V_{pred} ratio is equal to 0.99 for the training set and 1.02 for the validating set. The coefficients of variation are 12.79% and 12.53%. respectively As can be seen by comparison with Table 5.6, the network improves the correlation with the empirical

test for the training beams and for the unseen (validating) beams. Figure 5.17 shows the correlation of the ANN predictions for the 30 unseen beams.

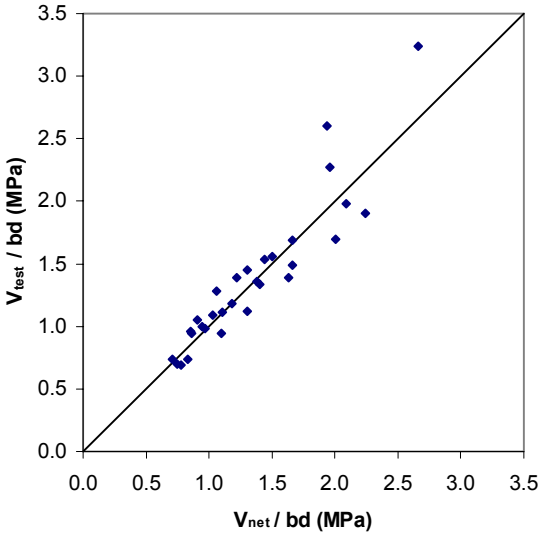

Figure 5.17: Artificial Neural Network for beams without web reinforcement. Correlation with 30 unseen beams (validating set).

Beam specimens	nº beams	Average V_{test} / V_{net}	COV (%) V_{test} / V_{net}
All	177	1.00	12.75
$d \geq 900$ mm	18	0.99	8.20
$d \leq 100$ mm	0	-	-
$\rho_l \leq 1\%$	37	1.01	9.01
$f_c > 50$ MPa	95	0.99	12.80
$f_c \leq 50$ MPa	82	1.00	12.73
$\rho_l > 2\%$ $f_c > 50$ MPa	57	0.98	14.02
$\rho_l > 2\%$ $f_c \leq 50$ MPa	34	1.00	13.59

Table 5.7: Artificial Neural Network for beams without web reinforcement. Verification using partial sets of the database.

To ensure that the correlation is satisfactory, a partial set analysis was carried out to study the influence of different parameters. This can be compared to the analyses in Table 5.4 for different shear procedures. The network performance is very similar for the different partial sets, as shown in Table 5.7.

5.4.3 Parametrical analyses based on the ANN results

After the network has been adequately trained, it is possible to implement the activation functions and the weights in a simple spreadsheet, and to generate new beams to study the influence of the different parameters which affect the failure shear strength.

Size effect. Influence of the effective depth, *d*.

As was mentioned in Chapter 2, as the depth of a beam is increased, its failure shear stress decreases. Moreover, Fujita et al. (2002) demonstrated that the size effect on the shear capacity is linked to the concrete compressive strength. Experimental tests they carried out showed that the shear fracture of HSC was characterised by a conspicuous crack localization as compared to ordinary strength concrete, and that the propagation of these cracks was rapid, resulting in a more brittle fracture. A study using Fracture Mechanics conducted by Fujita et al. to determine the relationship between size effect and concrete compressive strength led to the following expressions:

$$\frac{V}{bd} \propto 0.32\left(\frac{l_{ch}}{d}\right)^{1/4} \quad \text{for NSC} \tag{5.9a}$$

$$\frac{V}{bd} \propto 0.30\left(\frac{l_{ch}}{d}\right)^{1/2} \quad \text{for HSC} \tag{5.9b}$$

where l_{ch}, the characteristic length, is equal to:

$$l_{ch} = 30700 \cdot f_c^{-1.1} \tag{5.10}$$

The EHE shear procedure does not consider the size effect to be related to the compression strength. On the other hand, the ACI 11-3 expression does not take into account the size effect. These two procedures are compared in Figure 5.18 to the ANN predictions for a set of 10 beams with b = 200 mm, ρ_l = 2%, a/d = 3. Parameters d and f_c

varied as indicated in the graphs. The ACI 11-3 equation does not correlate properly with the test result, and for beams with a high effective depth it may be unconservative.

For normal strength concrete (f_c = 35 MPa) the EHE predictions show satisfactory agreement with the ANN results. Nevertheless, the size effect is under-estimated for HSC beams.

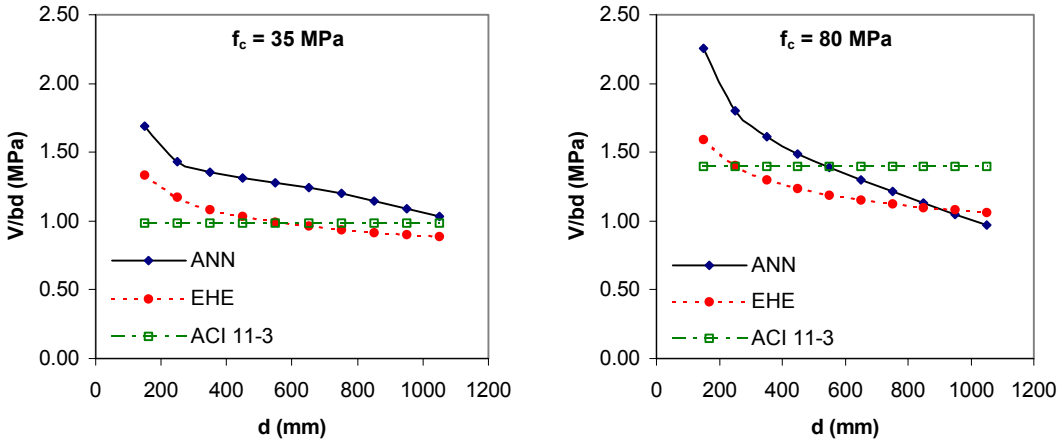

Figure 5.18: ANN results compared to the EHE and ACI 11-3 predictions for beams without web reinforcement. Size effect related to the concrete compressive strength.

If the size effect factor given in the EHE code is replaced with the factor given by Fujita et al. the curves correlate better, as shown in Figure 5.18, although it is slightly conservative for HSC beams. Besides, the Fujita equation is not continuous for different concrete compressive strengths, and this makes it difficult to implement it in a shear design procedure.

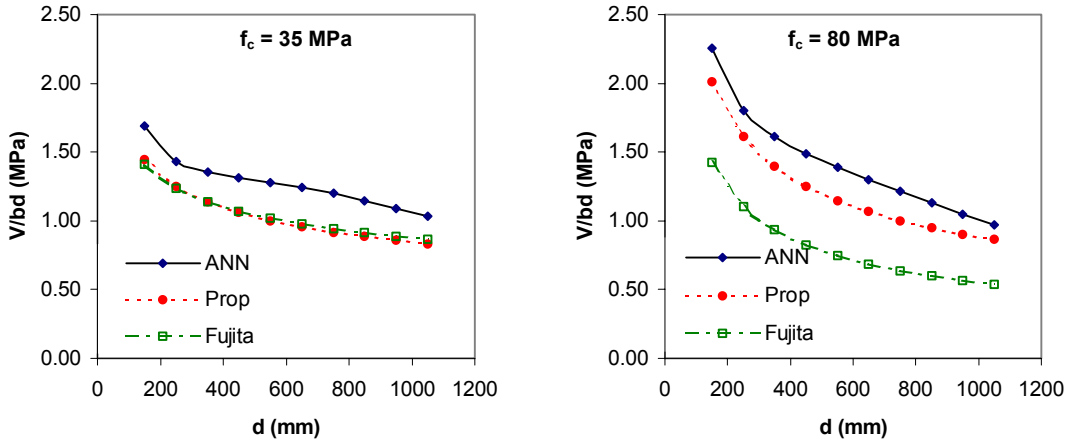

Figure 5.19: ANN results compared to the predictions made by Fujita's method and the method proposed in this section for beams without web reinforcement. The size effect as related to the concrete compressive strength.

A new size effect factor was developed using Fujita's and the Artificial Neural Network predictions to modify the current EHE procedure. Equation 2.5 will remain without any safety factor, as follows:

$$V_c = \left[0.15\xi\left(100\rho_s f_{ck}\right)^{1/3}\right] b_0 d \tag{5.11}$$

$$\xi = \left(\frac{150000 \cdot f_c^{-1.1}}{d}\right)^{0.25\left(1+\frac{f_c-25}{75}\right)} \tag{5.12}$$

The satisfactory agreement between this proposed equation and the ANN results is shown in Figure 5.19.

Influence of the concrete compressive strength, f_c.

In the last section the dependence of the size effect and the concrete compressive strength has been shown when studying the size effect for different concretes. However, it is possible to study the same problem from another point of view. Here the influence of the concrete compressive strength will be analysed for different beam depths. The conclusions will be the same as in the previous section.

Figure 5.20 plots the failure shear strength of a series of reinforced concrete beams without web reinforcement. The parameters f_c and d varied as indicated in the graphs. The web width, amount of longitudinal reinforcement and slenderness ratio were 200 mm, 2% and 3 respectively. For the 250 mm effective depth beam, the response is almost linear. The EHE procedure limits the concrete compressive strength to 60 MPa, leading to excessively conservative factors for HSC beams. However, for the 900 mm-effective depth series the shear strength increases until the concrete compressive strength reaches 50 MPa. For HSC beams, the increase in compressive strength produces a decrease in failure shear strength. The series in which d = 500 mm presents a intermediate behaviour.

Equation 5.11, proposed above, agrees with the ANN results as can also be seen in Figure 5.20.

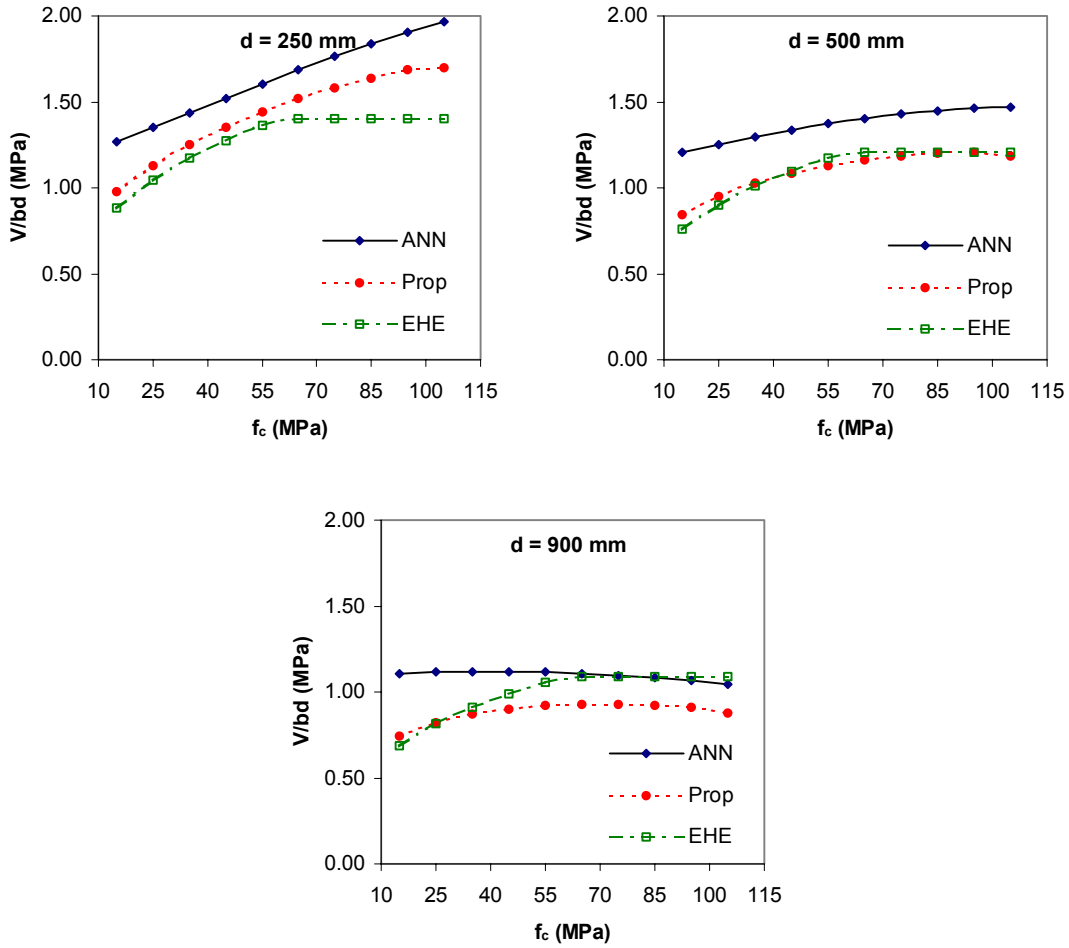

Figure 5.20: ANN results compared to the predictions made by the EHE and the method proposed in this section for beams without web reinforcement. Influence of the concrete compressive strength as related to the size effect.

It is the author's opinion that this behaviour may be explained as follows: the influence of the size effect becomes bigger when the concrete compressive strength increases, to such an extent that, for deep beams, the benefit of having a higher concrete compressive strength is lower than the loss caused by the size effect. This effect could probably be explained by using Fracture Mechanics.

Influence of the amount of longitudinal reinforcement.

The influence of the amount of longitudinal reinforcement predicted by the ANN results is analysed here and compared with the current EHE procedure and the ACI 11-3 equation.

The EHE shear procedure suggests that the influence of the amount of longitudinal reinforcement is proportional to $\rho^{1/3}$ and must to be limited to $\rho \leq 2\%$. On the other hand, the ACI 11-3 equation does not take into account its influence. This equation could give unconservative results for members with a low amount of longitudinal reinforcement, as was previously stated in §2.2.2.

The ANN predictions propose that the longitudinal reinforcement has a greater influence (Figure 5.21). Moreover, it would only be necessary to limit this value to 4% for both normal and high strength concrete. No significant difference has been found for different concretes or different beam depths. The beams analysed in Figure 5.21 were of the following dimensions: b = 200 mm, d = 300 mm, and a/d = 3. The longitudinal reinforcement and the concrete compressive strength varied as indicated in the graphs.

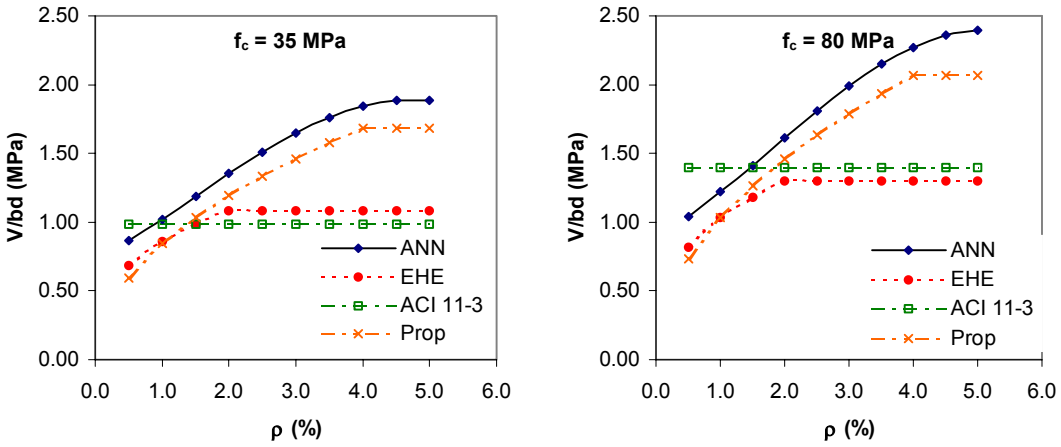

Figure 5.21: ANN results compared to the predictions made by the EHE and the method proposed in this section for beams without web reinforcement. Influence of the amount of longitudinal reinforcement.

In order to adapt the proposed equation 5.11 to take into account the higher influence of the longitudinal reinforcement, that term has been raised to a different power:

$$V_c = \left[0.13\xi\left(100\rho_s\right)^{1/2} f_c^{1/3}\right] b_0 d \qquad (5.13)$$

where $\rho_s \leq 0.04$, and ξ is defined in equation 5.12. It can be observed that the value limiting ρ_s could be related to the concrete compressive strength, since for high-strength concrete beams the limit would be higher than for normal-strength concrete beams.

The predicted values as calculated by this new equation are also shown in Figure 5.21.

Influence of the *a/d* ratio.

The weight this parameter exerts on the failure shear strength has been evaluated by previous authors. In fact, the Model Code formulation (equation 2.4 in this thesis) proposes a term to take it into account. Figure 5.22 plots the influence of *a/d* predicted by the Artificial Neural Network, and compares it with Model Code results, which show a satisfactory agreement. However, the EHE Code, which is based on the Model Code, omitted the term because of difficulties it caused in real beams with distributed loads.

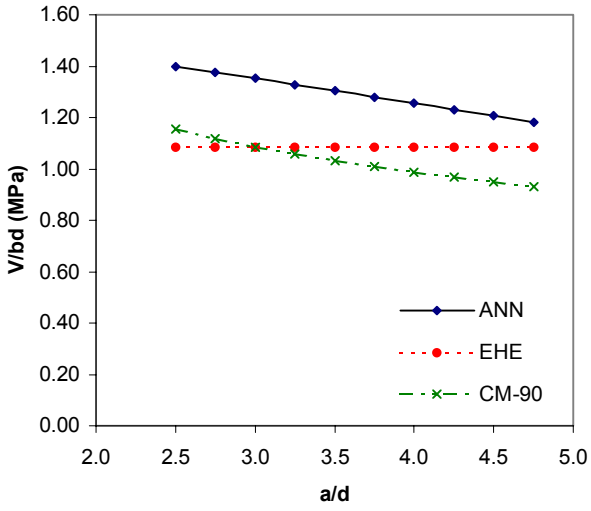

Figure 5.22: ANN results compared to EHE and CM-90 predictions for beams without web reinforcement. Influence of the a/d ratio.

5.5 Artificial Neural Network for members containing shear reinforcement

5.5.1 Data selection

The complete database for members with web reinforcement, described in §5.1, was that used for developing the ANN. Therefore, a total number of 123 test beams were utilized. These data were divided into two sets: a training set containing 104 beams, and a validating set comprised of 19 beams. The criteria for selecting the validating set were the same as were used for beams without web reinforcement (§5.4.1).

The input parameters used were the effective depth (*d*); the web slenderness factor *d/b*; where *b* is the web width; the *a/d* ratio; the reinforcement ratio of longitudinal tensile steel (ρ_l); the concrete cylinder compressive stress (f_c); and the amount of transverse reinforcement expressed in MPa (ρ_w). The output value is the failure shear strength (V). Table 5.8 summarises the ranges of the different variables.

Parameter	Minimum	Maximum
d (mm)	198	925
d/b	0.792	4.5
ρ_l (%)	0.50	5.80
ρ_w (%)	0.33	3.57
f_c (MPa)	21	125.2
a/d	2.49	5.00
V (KN)	63.28	1172.19

Table 5.8: Artificial Neural Networks for beams with web reinforcement. Ranges of parameters in the database.

The correlation of the two sets with the different shear procedures is shown in Table 5.9. For elements with web reinforcement, agreement with the Response-2000 results was slightly better for the training set. All the information pertaining to the test beams in both sets is summarised in Annex C.

Beam specimens	nº beams	Average V_{test} / V_{pred}						COV V_{test} / V_{pred} (%)					
		EHE	EC-2	AASHTO	ACI11-5	ACI11-3	Resp	EHE	EC-2	AASHTO	ACI11-5	ACI 1-3	Resp
Training set	104	1.65	1.84	1.19	1.37	1.41	1.07	26.31	39.36	19.06	24.92	26.95	16.74
Validating set	19	1.60	1.76	1.15	1.32	1.36	1.07	26.50	46.43	20.51	22.98	25.63	21.08

Table 5.9: Artificial Neural Networks for beams with web reinforcement. Training and validating sets.

5.5.2 Topology of the Artificial Neural Network, learning process and validation

The parameters fixed before building the Artificial Neural Network were:

- 6 neurons in the input layer (*d, d/b, a/d,* ρ_l, ρ_w, and f_c).
- 1 neuron in the output layer (*V*).
- Feed-forward connections, based on other authors' experience.

- Activation function: Sigmoid transfer function (Figure 5.13).
- Momentum: 0.9.
- Pattern training.

The trial and error process took more than 65 attempts. The optimum solution was obtained after 3000 epochs with a neural network containing 9 hidden units. The learning rate varied to ensure convergence between 0.175 at the beginning of the training procedure and 0.15. The final weights and biases that fully define the ANN are given in Annex D.

The average V_{test}/V_{pred} ratio is equal to 1.00 for the training set and 1.01 for the validating set. The coefficients of variation are 10.96% and 13.38% respectively. A partial set analysis was also carried out to study the agreement between different sets of beams. This is shown in Table 5.10 and can be compared to the analyses in Table 5.4 for different shear procedures.

Beam specimens	nº beams	Average V_{test} / V_{net}	COV (%) V_{test} / V_{net}
All	123	1.00	11.32
$d \geq 750$ mm	12	1.01	10.63
$\rho_w \leq 1$MPa	93	1.00	11.19
$\rho_w > 1$MPa $\rho_w \leq 2$MPa	23	1.02	12.11
$\rho_w > 2$MPa	7	0.96	10.53
$f_c \leq 50$ MPa	38	1.00	12.48
$f_c > 50$ MPa	85	1.01	10.84
$\rho_l \leq 2$ %	19	1.01	10.52

Table 5.10: Artificial Neural Network for beams with web reinforcement. Verification using partial sets of the database.

The coefficient of variation of the V_{test}/V_{pred} ratio is very similar for the different subsets. However, the average is somewhat unconservative for highly reinforced members (ρ_w > 2 %).

5.5.3 Parametrical analyses based on the ANN results

Once the Artificial Neural Network has been trained, a parametric analysis was used to study the influence of the different parameters having an effect on the failure shear strength of members with web reinforcement. The parametric study used entailed many more difficulties than the parametrical analysis for members without web reinforcement for three basic reasons:

- It presented a new variable: the amount of transverse reinforcement, which interacts considerably with the other parameters,
- The number of test beams was not very high and there was a lack of information for some groups of beams (i.e. highly reinforced beams for which *d* was greater than 600 mm), and
- Comparison can only be made with the failure shear strength independently of the concrete and steel contributions. For this last reason, it is not possible to directly formulate a design equation, as it is necessary to divide by both contributions.

Influence of the amount of web reinforcement

Logically, the amount of web reinforcement has a very important influence on the failure shear strength. Historically, from the first models of Ritter and Mörsch to variable-angle-truss-models with or without concrete contribution, linearity has been assumed to exist between the amount of shear reinforcement and the ultimate beam response (§2.3.2). Nevertheless, some authors pointed out that for high-strength concrete beams stirrups seemed to be more effective.

The Artificial Neural Network predicts a non-linear response based on the amount of web reinforcement. The greater number of stirrups the less effective they are, as can be seen in Figure 5.23. This effect leads to unconservative results, compared to the ANN results, for highly reinforced concrete beams calculated by the EHE or EC-2 procedures.

It agrees with the correlation shown in Table 5.4 for beams containing an amount of web reinforcement higher than ρ_w > 2 MPa. The AASHTO procedure takes into account compatibility and its predictions correlate better with the ANN results.

The beam specimens from Figure 5.23 had the following characteristics: d = 350 mm, b = 200 mm, ρ_l = 3 % and a/d = 3. The parameters f_c and ρ_w varied as indicated in the plots.

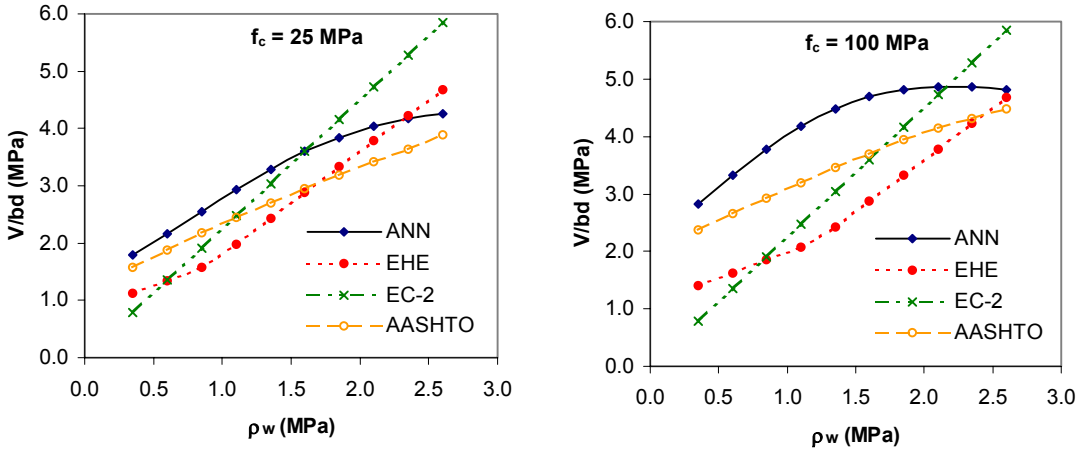

Figure 5.23: ANN results compared to the EHE, EC-2 and AASHTO predictions for beams with web reinforcement. Influence of the amount of shear reinforcement in relation to the concrete compressive strength.

As was mentioned in Chapters 2 and 4, the influence of the stirrups depends on the concrete compressive strength. For HSC beams that are not highly reinforced, this influence is higher than for normal strength concrete beams, according to the ANN results. This is the reason for the steeper slope of the f_c = 100 MPa graph. Neither the EHE, EC-2, or AASHTO procedures reproduce this behaviour.

Size effect. Influence of the effective depth, *d*.

To study the size effect using the Artificial Neural Network we must take certain precautions because of the lack of heterogeneity of the database. The percentage of test beams with web reinforcement in which d is greater than 900 mm is only 5.7%, compared to 10.2% for beams without web reinforcement. However, the percentage of experimental beams in which d greater than 500 mm is equal to 25.2%. For this reason the size effect will be studied for effective depths of up to 700 mm.

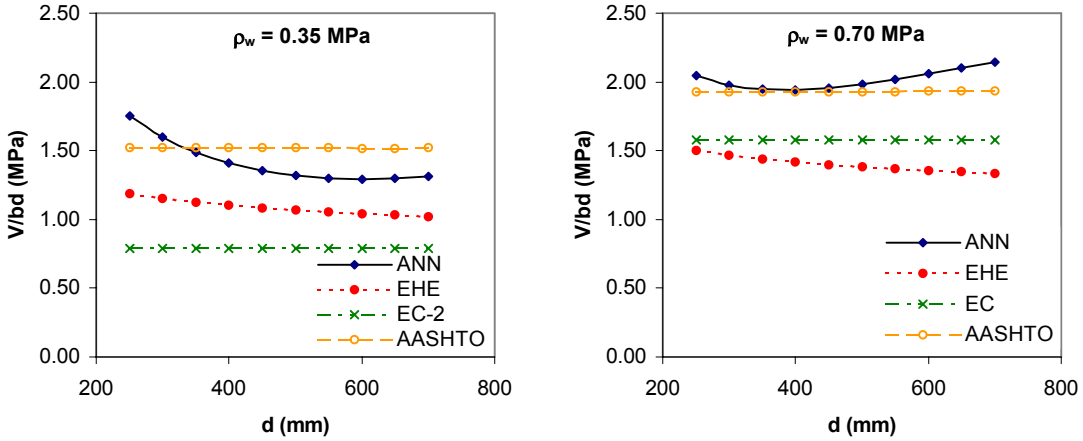

Figure 5.24: ANN results compared to the EHE, EC-2 and AASHTO predictions for beams with web reinforcement. Size effect in relation to the amount of shear reinforcement.

Collins (1997) pointed out that for members with a low amount of web reinforcement a reduction in failure shear stress was detected. This effect decreased when the amount of shear reinforcement increased.

The ANN analysis reveals that for lowly shear-reinforced members (b = 300 mm, f_c = 25 MPa, ρ_w = 0.35 MPa, ρ_l = 2.5 %, and a/d = 3) the size effect may reduce the failure shear stress about 25% as effective depth is increased from 250 mm to 700 mm, as is shown in Figure 5.24. Members with twice this amount of shear reinforcement, the second series in Figure 5.24, do not show any reduction in shear strength due to the size effect in the ANN analysis. Moreover, analyses carried out on beams with higher shear reinforcement present a contrary effect. However, it is the author's opinion that there is not experimental evidence of this fact, and as it is difficult to explain it analytically, and it could be the focus of a future experimental campaign.

How the influence of the size effect is weighed by some current codes of practice is also shown in the previous figure. The AASHTO and EC-2 procedures do not take it into account. The EHE equations consider the influence of the size effect, but only for low reinforced members, as for highly transversal reinforced beams, the steel contribution is higher than the concrete contribution and only the first term is used with $cot\theta = 2$ (see §2.3.6).

Influence of the concrete compressive strength, f_c.

The influence of the concrete compressive strength depends on the beam size and the amount of transverse reinforcement.

Figure 5.25 plots the failure shear strength in relation to the concrete compressive strength. The beams concerned the following characteristics: b =300 mm, a/d = 3, ρ_l = 3%, and ρ_w = 0.50 MPa. The effective depth and the concrete compressive strength varied as indicated in the graphs.

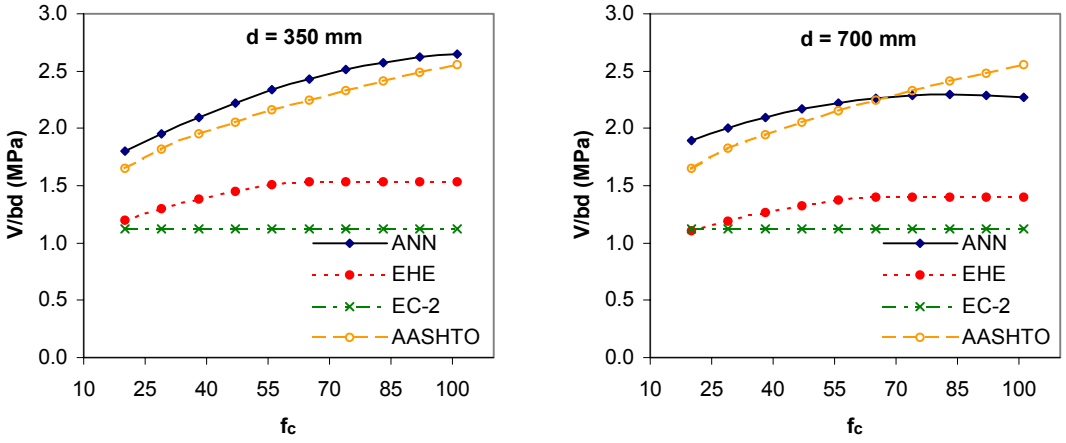

Figure 5.25: ANN results as compared to the EHE, EC-2, and AASHTO predictions for beams with web reinforcement. Influence of the concrete compressive strength in relation to the beam size.

From the above graphs, the influence of the concrete compressive strength decreases for the d = 700 mm beam specimens in comparison to the d = 350 mm series. The EHE procedure is very conservative, and it does not give a satisfactory reproduction of the behaviour for the small beams. The concrete compressive strength should not be limited to 60 MPa, at least for small beams. However, this limitation could be acceptable for deep beams. On the other hand, the EC-2 procedure does not take into account the influence of f_c, as is shown in Figure 5.25. The AASHTO Specifications offer the best correlation.

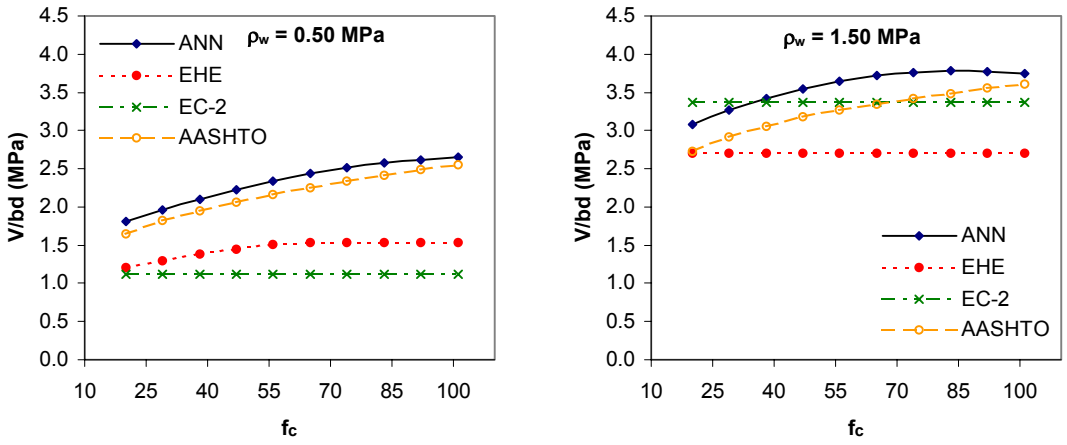

Figure 5.26: ANN results as compared to the EHE, EC-2 and AASHTO predictions for beams with web reinforcement. Influence of the concrete compressive strength in relation to the amount of transverse reinforcement.

The relationship between the concrete compressive strength and the amount of transverse reinforcement is shown in Figure 5.26 for two series of beams in which d is equal to 350 mm, b = 300 mm, a/d = 3, and ρ_l = 3 %.

For normal strength concrete beams, the greater the amount of transversal reinforcement, the higher the influence of the concrete compressive strength. The AASHTO procedure shows a satisfactory adaptation to this trend. However, for highly-reinforced high-strength concrete beams there is a maximum strength around 85 MPa concrete.

Influence of the amount of longitudinal reinforcement.

In the EHE procedure (§2.3.6), the influence of the amount of longitudinal reinforcement depends indirectly on the amount of transversal reinforcement. For highly reinforced concrete members, the EHE equations only consider the steel contribution in which $cot\theta$ = 2 (β = 0). Therefore, the influence of the amount of longitudinal reinforcement in not felt in these beams. On the other hand, for lowly-reinforced concrete beams, the failure shear strength is the sum of the concrete and steel contributions, and the influence of the amount of flexural reinforcement is considered to be up to 2% of this reinforcement.

However, based on experimental tests, the Artificial Neural Network predicts that the flexural reinforcement will have a greater influence on both beams with high and beams with low reinforcement, as can be seen in Figure 5.27. No limitation seems necessary for amounts up to 5%.

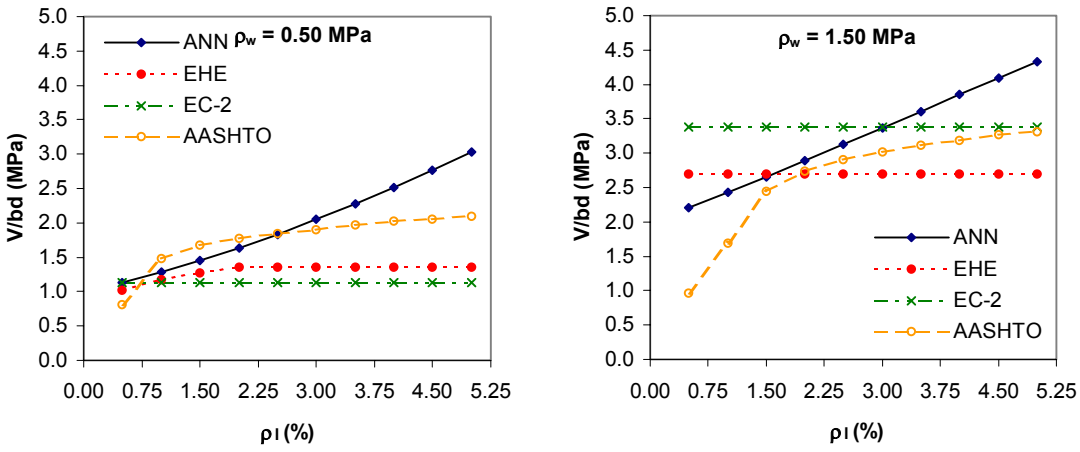

Figure 5.27: ANN results as compared to the EHE, EC-2, and AASHTO predictions for beams with web reinforcement. Influence of the amount of longitudinal reinforcement.

Influence of the a/d ratio.

The influence of the a/d ratio, or the M/V relationship, is not taken into account in most codes of practice. The AASHTO LRFD procedure is an exception and, as one can see in Figure 5.28, it predicts lower failure shear stress values for higher M/V relationships. In the series of beams shown in the figure, b = 300 mm, d= 500 mm, f_c = 35 MPa, ρ_l = 3 % and ρ_w = 1 MPa.

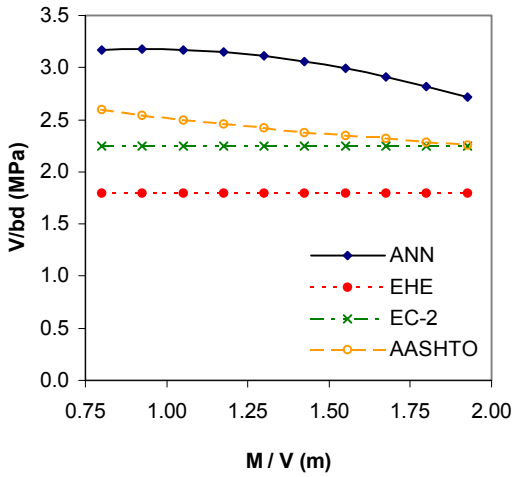

Figure 5.28: ANN results as compared to the EHE, EC-2 and AASHTO predictions for beams with web reinforcement. Influence of the moment/shear (M/V) relationship.

5.6 Conclusions of the analyses of 316 test beams

The experimental results obtained in 316 beams tested in different laboratories around the world have been compared with the failure shear strength predicted by the EHE code, Final Draft of Eurocode 2 (2002), AASHTO LRFD Specifications, and Response 2000 program. The behaviour of each code have been carefully underlined.

Moreover, two Artificial Neural Networks have been developed to predict the empirical results, and a parametric study have been carried out based on the Artificial Neural Network predictions.

In the next chapter the main conclusions of these analyses will be summarised in order to propose a new shear design method.